Huygens's Clocks

Matthew Bennett; Michael F. Schatz; Heidi Rockwood; Kurt Wiesenfeld

Huygens's clocks

By Matthew Bennett[1], Michael F. Schatz[1],
Heidi Rockwood[2] and Kurt Wiesenfeld[1]

[1]Center for Nonlinear Science and School of Physics and
[2]School of Modern Languages, Georgia Institute of Technology,
Atlanta, GA 30332-0430, USA

The 336-year-old synchronization observations of Christiaan Huygens are re-examined in modern experiments. A simple model of synchronization is proposed.

1. Introduction

Shortly after The Royal Society's founding in 1660, Christiaan Huygens, in partnership with the Society, set out to solve the outstanding technological challenge of the day: the longitude problem, i.e. finding a robust, accurate method of determining longitude for maritime navigation (Yoder 1990). Huygens had invented the pendulum clock in 1657 (Burke 1978) and, subsequently, had demonstrated mathematically that a pendulum would follow an isochronous path, independent of amplitude, if cycloidal-shaped plates were used to confine the pendulum suspension (Yoder 1990). Huygens believed that cycloidal pendulum clocks, suitably modified to withstand the rigours of sea travel, could provide timing of sufficient accuracy to determine longitude reliably. Maritime pendulum clocks were constructed by Huygens in collaboration with one of the original fellows of The Royal Society, Alexander Bruce, 2nd Earl of Kincardine. Over the course of three years (1662–1665) Bruce and the Society supervised sea trials of the clocks. Meanwhile, Huygens, remaining in The Hague, continually corresponded with the Society through Sir Robert Moray, both to inquire about the outcome of the sea trials and to describe the ongoing efforts Huygens was making to perfect the design of maritime clocks. On 1 March 1665, Moray read to the Society a letter from Huygens, dated 27 February 1665, reporting of (Birch 1756)

> an odd kind of sympathy perceived by him in these watches [two maritime clocks] suspended by the side of each other.

Huygens's study of two clocks operating simultaneously arose from the practical requirement of redundancy for maritime clocks: if one clock stopped (or had to be cleaned), then the other could be used to provide timekeeping (Huygens 1669). In a contemporaneous letter to his father, Huygens further described his observations, made while confined to his rooms by a brief illness. Huygens found that the pendulum clocks swung in exactly the same frequency and 180° out of phase (Huygens 1950a, b).

When he disturbed one pendulum, the anti-phase state was restored within half an hour and remained indefinitely.

Motivated by the belief that synchronization could be used to keep sea clocks in precise agreement (Yoder 1990), Huygens carried out a series of experiments in an effort to understand the phenomenon. He found that synchronization did not occur when the clocks were removed at a distance or oscillated in mutually perpendicular planes. Huygens deduced that the crucial interaction came from very small movements of the common frame supporting the two clocks. He also provided a physical explanation for how the frame motion set up the anti-phase motion, but though his prowess was great his tools were limited: his discovery of synchronization occurred in the same year when young Isaac Newton removed to his country home to escape the Black Plague, and begin the work that eventually led to his *Principia*, published some 20 years later.

The Royal Society viewed Huygens's explanation of synchronization as a setback for using pendulum clocks to determine longitude at sea (Birch 1756).

> Occasion was taken here by some of the members to doubt the exactness of the motion of these watches at sea, since so slight and almost insensible motion was able to cause an alteration in their going.

Ultimately, the innovation of the pendulum clock did not solve the longitude problem (Britten 1973). However, Huygens's synchronization observations have served to inspire study of sympathetic rhythms of interacting nonlinear oscillators in many areas of science. The onset of synchronization and the selection of particular phase relations is a fundamental problem of nonlinear dynamics and one which has been avidly pursued in recent years in problems ranging from neurobiology and brain function (Rodriguez *et al.* 1999) to animal locomotion (Strogatz & Stewart 1993; Golubitsky *et al.* 1999), superconducting electronics, laser physics, and smart antenna arrays (Liao & York 1993).

In this paper we reconsider Huygens's observations. To our knowledge, previous attempts to understand Huygens's observations are few and ultimately unsatisfactory. We have built an updated version of the two-clock system, with pendulums attached to a common frame free to move in one dimension. In our experiments, we vary the coupling strength by changing the ratio of pendulum mass to system mass μ, and, thereby, explore in greater depth the situation facing Huygens. At small μ (weak coupling) corresponding to Huygens's situation, we find that whenever the pendulums frequency lock, they fall into anti-phase oscillations. However, as the coupling is increased by increasing μ, we observe another state in which one or both clocks cease to run: a state we call 'beating death'. This behaviour is increasingly dominant as μ becomes large. Thus, our results suggest Huygens's observations depended somewhat serendipitously on the extra heavy weighting of his clocks intended to make them more stable at sea.

We study the problem theoretically by deriving a Poincaré map for the nonlinear dynamics. Our map is in agreement with the experimental observations; moreover, in one useful limit, the map reduces to a single degree of freedom, and captures many essential results of our experiments. We are also able to explain the behaviour in very direct physical terms based on a normal mode description, a picture originally put forward by Korteweg (1906).

2. Background

(a) Details of Huygens's clock experiments

The operation of a pendulum clock is described in great detail by Huygens (Huygens 1986). In brief, the pendulum is attached to an escapement, which alternately blocks and releases a scape wheel as the pendulum oscillates. This action provides the timing that is transmitted from the scape wheel to the clocks' hands via a gearing system (the *motion work*). The scape wheel is also connected through a separate gearing system (the *going train*) to an energy source, typically a wound spring or elevated weights. The unwinding spring or falling weights drive the motion of the scape wheel, which, in turn, provides small 'kicks' to the pendulum via the escapement. This transmission of energy to the pendulum compensates for losses due to friction; thus, the pendulum continues to oscillate indefinitely as long as the spring is periodically rewound or the fallen weights are periodically raised back up.

Many experimental details of Huygens's observations are recorded in his writings (Huygens 1950a, b; Huygens 1986). The pendulum in each clock measured *ca.* 9 in† in length, corresponding to an oscillation period of *ca.* 1 s. Each pendulum weighed $\frac{1}{2}$ lb‡ and regulated the clock through a verge escapement, which required each pendulum to execute large angular displacement amplitudes of *ca.* 20° or more from vertical for the clock to function (see Rawlings (1944) and also Landes (1983, appendix A) for a detailed description of the verge escapement). The amplitude dependence of the period in these clocks was typically corrected by use of cycloidal-shaped boundaries to confine the suspension (Huygens 1986). Each pendulum clock was enclosed in a 4 ft¶ long case; a weight of *ca.* 100 lb was placed at the bottom of each case (to keep the clock oriented aboard a ship.) From this information, we estimate that the important experimental parameter μ, the ratio of the single pendulum mass to the total system mass, is *ca.* 0.005. Though the two clocks differed in certain physical aspects, (for example, Huygens notes that the size of the clocks was somewhat different (Huygens 1950a, b)) the clocks were closely matched in those characteristics we expect are essential for the dynamics. In particular, well-adjusted pendulum clocks of the 1660s would typically run at rates which differed by only 15 s per day (so their natural frequencies differed by approximately two parts in 10 000) (Landes 1983). Pendulum clocks represented a tremendous advance in horology, the science of timekeeping. Before Huygens's invention of the pendulum clock, typical clocks (e.g. verge escapement with balance wheel regulator) varied by *ca.* 15 min (1%) per day (Landes 1983).

Huygens's laboratory notebook contains a detailed description of tests and observations on synchronization (Huygens 1950a, b). In some experiments, Huygens studied two clocks that were suspended side by side, each hanging from a hook embedded in the same wooden beam. In other experiments, Huygens studied a configuration with each clock hanging from its own wooden beam and the two beams lying on top of back to back chairs. At first, Huygens suspected the 'sympathy' was due to induced air currents, but eventually concluded the cause was the 'imperceptible movements' of the common supporting structure. The associated coupling was weak: when Huygens disturbed the pendulums, he found the clocks required *ca.* 30 min

---

† 1 in equals 2.54 cm.

‡ 1 lb equals 0.4536 kg.
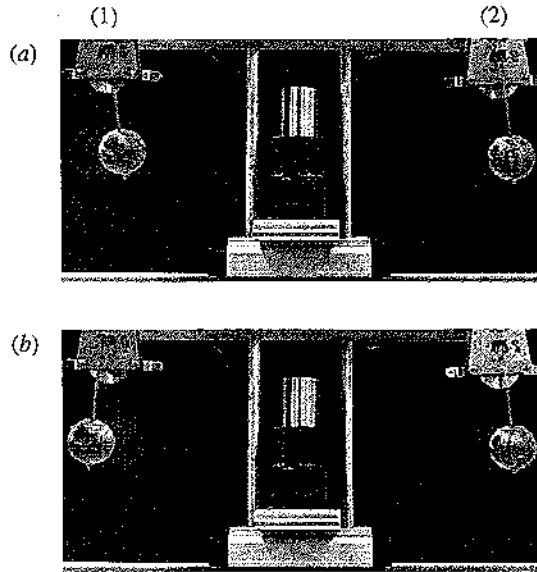
¶ 1 ft equals 12 in equals 30.5 cm.

Figure 1. Multiple-exposure images illustrate the anti-phase attractor of a large mass ratio ($\mu = 0.0063$) system of two pendulums mounted on a common translating beam. (*a*) The system is started with equal amplitude, in-phase oscillation of the left (1) and the right (2) pendulums. In the presence of weak coupling through lateral motion of the mounting cart, the in-phase state is unstable and, after a sufficient time, the system oscillates stably in anti-phase final state (*b*).

before synchronization was restored. At one second per cycle, a transient time of 30 min amounts to 1800 cycles. (Interestingly, Huygens considers this restoration time as fast, perhaps a reflection of the pace of life then and now.) The dissipation was also weak, as can be seen from the following estimate: the total energy available to run each clock is *ca.* 100 J, obtained from weights of *ca.* 10 kg mass falling a distance of 1 m. Assuming this energy is sufficient to keep a clock running for *ca.* 250 000 oscillations (*ca.* 3 days), the energy input per oscillation is *ca.* 4×10^{-4} J. The total energy in a 9 in long, $\frac{1}{2}$ lb pendulum swinging through a semiarc of $25°$ is *ca.* 0.05 J. Thus, energy loss per oscillation relative to the pendulum energy is *ca.* 0.8%.

(*b*) *Recapping Korteweg and Blekhman studies*

We know of two studies which were directly motivated by Huygens's observations. The first was Korteweg's (1906) paper in which he analysed a three-degree-of-freedom model consisting of two plane pendulums connected to a rigid frame free to oscillate in one dimension. (Korteweg was also strongly motivated by the 18th century observations of Ellicott regarding the slow beating between weakly coupled pendulums.) Korteweg made a linear normal mode analysis for small oscillations in the absence of damping and driving effects. To explain why only certain of these modes might be observed, and others not, Korteweg introduced the idea that *friction* is responsible for certain motions being unsustainable. If a mode involved large-amplitude motion of the supporting frame, he argued, the internal clock mechanisms would be unable to provide enough energy to sustain this motion. Conversely, for a mode in which the frame moved only a little, the energy input could overcome the effects of friction.
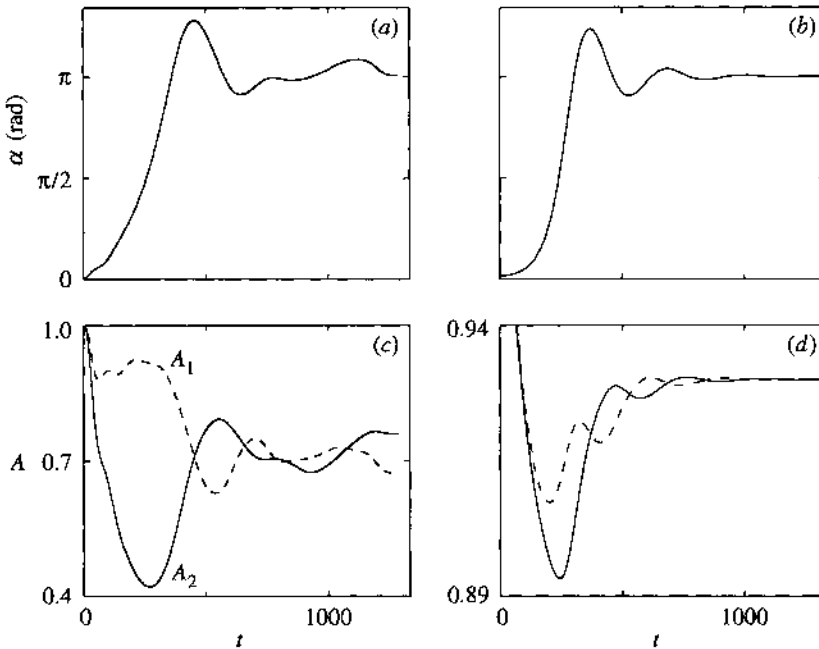
Figure 2. (*a*), (*b*) Time-series from pendulum experiments and (*c*), (*d*) simulations illustrating the evolution from unstable in-phase to stable anti-phase oscillations. Damped beating is found in both the pendulums' (*a*), (*c*) phase difference α and (*b*), (*d*) amplitudes A_1, A_2. Time is scaled by the pendulum period and amplitudes are scaled by the initial amplitude at $t = 0$. The experimental conditions correspond to those listed in figure 1.

Though these aspects of energy damping and energy input were not included in his quantitative analysis, Korteweg concluded that Huygens's observations were entirely captured by the three-degree-of-freedom model, and that the anti-phase mode, if not the only sustainable motion, enjoyed a distinct advantage over in-phase motion. This advantage was cleverly used in a different context for precise measurements of the acceleration of gravity by Vening Meinesz and others, who used pairs of pendulums set into free (no driving) anti-phase oscillation (Heiskanen & Vening Meinesz 1958).

Blekhman (1988) also discusses Huygens's observations in his book, and he recounts the results of a laboratory reproduction of the coupled clocks as well as presenting a theoretical analysis of oscillators coupled through a common supporting frame. His model is similar to the one studied by Korteweg, except that Blekhman uses van der Pol oscillators rather than pendulums, so that his quantitative analysis includes both (weak) driving and damping effects. Blekhman was primarily motivated by the general aspects of synchronization phenomena found in a wide variety of physical systems, and it is probably for this reason that he chose to use van der Pol oscillators. He predicted that both in-phase and anti-phase motions are stable under the same circumstances (that is, the two are coexisting attractors). Somewhat puzzling is that he reports observing both states in the experimental reproduction: while this agrees with his predictions for the van der Pol system, Huygens (so far as we know) never mentioned stable in-phase synchronization.

3. Experimental realization and results

We re-examine Huygens's synchronization observations in an experiment with two pendulum clocks mounted side by side on a single wooden beam (figure 1). The pendulum clocks are commercially available spring-wound time pieces (Model 771-000, Uhrenfabrik Franz Hermle & Sohn, Gosheim, Germany). Each clock contains a 14.0 cm pendulum (with a nominal frequency of 1.33 Hz) of mass $m = 0.082$ kg; the pendulum is coupled to an anchor escapement, which enables the clock movement to function with small angular displacements of *ca.* $8°$ from vertical. The beam is mounted on a low-friction wheeled cart (Model ME-9454, Pasco Scientific, Roseville, CA). The combined system of clocks, beam and cart is placed atop a slotted track (ME-9429A, Pasco Scientific), which permits the system to translate freely in a direction parallel to the beam. The total mass of the cart and clocks without the pendulums is M. Weights are added to and removed from the cart to change M and, thereby, to change the system mass ratio $\mu \equiv m/(2m + M)$. The motion of each pendulum is monitored by tracking a laser beam reflected from the pendulum suspension using a position-sensing detector (Model 1L30, On-Trak Photonics, Lake Forest, CA). The lasers and detectors (not shown in figure 1) are mounted on the system, permitting measurement of each pendulum's angular position in the system reference frame. The voltage signal from each detector is recorded using a computer-based data-acquisition system; complex demodulation of the signals yields measurement of each pendulum's oscillation amplitude, frequency and phase as a function of time.

The clocks synchronize in anti-phase when the system mass ratio μ is comparable with that reported by Huygens (figures 1 and 2). In this case, the anti-phase state is the attractor when the system begins from any 'good' initial condition, which ensures that each clock is initially functioning. (Starting one pendulum at rest with zero angular displacement is an example of a 'bad' initial condition; the energy exchange between the coupled pendulums is not sufficient to jump-start a pendulum whose initial amplitude is too small to engage the escapement.) Consider, for example, the case where the system starts at rest with both pendulums having equal amplitude, in-phase angular displacements (figure 1). The approach to the anti-phase state is slow, occurring over the course of several hundred pendulum oscillations (figure 2a). The phase difference $\alpha = \alpha_1 - \alpha_2$ exhibits some overshoot, and small, slow variations in α about π persist indefinitely. The complex demodulated pendulum amplitudes A_1 and A_2 initially exhibit slow, approximately out-of-phase oscillations in a manner characteristic of beating between weakly coupled linear oscillators (figure 2b). These beating oscillations are damped and, eventually, the amplitudes become nearly steady and approximately equal as α gets close to π. During this evolution, the amplitude of the cart's motion is typically very small (*ca.* 0.1 mm).

Stable anti-phase synchronization requires the pendulum clocks to be very closely matched in frequency. For example, anti-phase synchronization is observed with $\mu = 0.0063$ when the difference between the natural frequencies of the clocks is 0.0009 Hz. By simply exchanging the pendulum bobs between these two (very similar but not identical) clocks, this frequency difference is increased to 0.0045 Hz and anti-phase synchronization no longer occurs. Instead, the two clocks run 'uncoupled' at their individual frequencies.
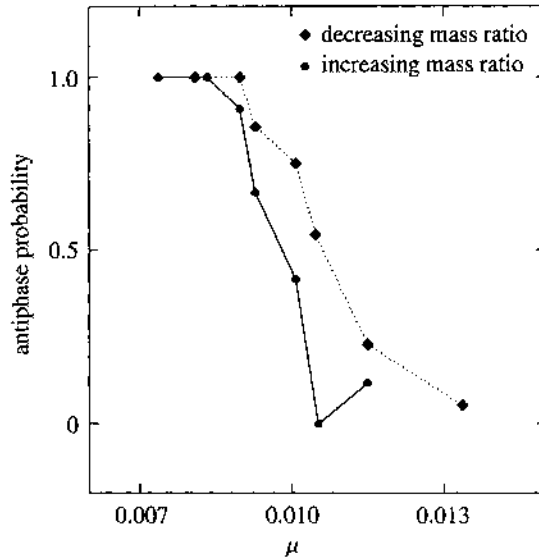
Figure 3. Probability of observing stable anti-phase oscillations as a function of mass ratio μ for the clock system that begins at rest with both pendulums having in-phase angular displacements of equal amplitude. In this range of μ only two asymptotic states are observed: anti-phase oscillation and beating death.

When μ is sufficiently increased, we find that some initial conditions can lead to a state, which we call 'beating death', where one or both of the clocks cease to function (figure 3). If the angular displacement of either pendulum clock falls below a minimum threshold, the escapement mechanism can no longer engage, the pendulum seizes, and the clock stops. When the pendulums start from rest with in-phase angular displacements of equal amplitude, anti-phase oscillations are always observed for $\mu < 0.0083$, while the clocks typically stop for $\mu > 0.0125$. At intermediate values of μ, either state may be the attractor of the system, depending on slight differences in the initial conditions. Additionally, as a function of μ, the system exhibits hysteresis, which may be due in part to the dependence of the track friction on the mass loading of the system.

We believe that our clock system contains the same essential ingredients as Huygens's clock system. In both cases, the clocks are mounted on a common support whose motion provides weak coupling. Dissipation is also weak both in Huygens's clocks and ours; in our case, we estimate the relative energy loss per oscillation is *ca.* 3%. Both systems of clocks are kept out of equilibrium by the inherently nonlinear driving from small impulsive kicks applied by the escapement mechanisms when the pendulums' displacement amplitudes exceed a threshold value. Of course, Huygens's clocks differ in certain details that are qualitatively unimportant as follows.

(a) Huygens's clocks were driven by falling weights; ours are spring driven.

(b) Huygens's clocks used a verge escapement, which required large displacements amplitudes of *ca.* 25° to function; our clocks use a newer (invented in the 1670s) anchor design, which enables clocks to function with smaller amplitudes.

(c) The length of Huygens's oscillating pendulums was continually varied by confining the suspension of each pendulum between cycloidal-shaped boundaries; our pendulums oscillated with a fixed suspension length.

4. Theory: model and analysis

We consider the three-degree-of-freedom model depicted in figure 4. Two plane pendulums hang from a common rigid frame which is constrained to move in one dimension. The pendulums are identical, each consisting of a point mass hanging from a massless rigid rod. In the absence of damping and driving, the Lagrangian is

$$\mathcal{L} = \tfrac{1}{2}(M + 2m)\dot{X}^2 + m\dot{X}\ell(\cos\phi_1\dot{\phi}_1 + \cos\phi_2\dot{\phi}_2) + \tfrac{1}{2}m\ell^2(\dot{\phi}_1^2 + \dot{\phi}_2^2)$$
$$+ mg\ell(\cos\phi_1 + \cos\phi_2) - \tfrac{1}{2}KX^2, \quad (4.1)$$

where ϕ_k is the angular displacement of the kth pendulum about its pivot point, X is the linear displacement of the platform, m is the pendulum mass, M is the platform mass, g is the acceleration due to gravity, ℓ is the pendulum length, and the overdot denotes differentiation with respect to time. We take the platform motion to be weakly bound by a harmonic restoring force, since in Huygens's experiments the common supporting beam was confined. In our experiments the platform is free to slide, so that $K = 0$. (In earlier experiments we included a confining force by mounting magnets on the platform base. The results were similar and for practical simplicity we finally settled on the $K = 0$ design.) In the analysis to follow, we keep the harmonic restoring force to handle both cases, and to check that this difference is indeed a minor detail.

We also add viscous damping to the pendulums and the platform, and a driving mechanism to model the clocks escapements. The governing equations of motion become

$$\ddot{\phi}_k + b\dot{\phi}_k + \frac{g}{\ell}\sin\phi_k = -\frac{1}{\ell}\ddot{X}\cos\phi_k + \tilde{f}_k, \quad (4.2)$$

$$(M + 2m)\ddot{X} + B\dot{X} + KX = -\sum_j m\ell(\sin\phi_k)^{\cdot\cdot}, \quad (4.3)$$

where b and B are friction coefficients. The clock mechanism, represented by $\tilde{f}_k$, provides the energy needed to keep the clock running (see below).

It is convenient to write the differential equations in dimensionless form, introducing a scaled position $Y = X/\ell$ and time $\tau = t\sqrt{g/\ell}$, so that

$$\phi_k'' + 2\gamma\phi_k' + \sin\phi_k = -Y''\cos\phi_k + f_k, \quad (4.4)$$

$$Y'' + 2\Gamma Y' + \Omega^2 Y = -\mu(\sin\phi_1 + \sin\phi_2)'', \quad (4.5)$$

where $\gamma = b\sqrt{\ell/4g}$, $\Gamma = B\sqrt{\ell/4g}/(M + 2m)$, $\Omega^2 = K/(M + 2m)$, $\mu = m/(M + 2m)$, and the prime denotes differentiation with respect to τ. The system mass ratio $\mu = m/(M + 2m)$ controls the coupling strength and is a key parameter in our analysis.

Rather than develop a detailed model of the escapement mechanism (Lepschy *et al.* 1992), we use a simple impulse rule: when the pendulum reaches a threshold angle $\pm\Phi$, the angular velocity reverses direction and its magnitude changes according to
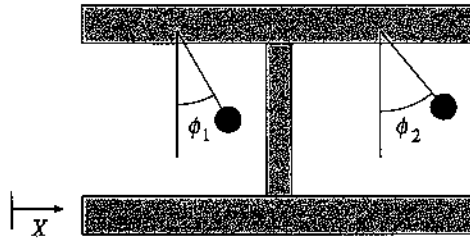
$$|\phi_k'| \to (1 - c)|\phi_k'| + \epsilon, \quad (4.6)$$

Figure 4. Sketch of model coupled-pendulum system.

where c and ϵ are small positive constants. Our choice of impulse rule is loosely based on the two-part action of the escapement, which first engages at a fixed angle and then delivers a kick on the downswing as the anchor hits. Since we are interested in the heavy platform limit $M \gg m$, we ignore the reaction force on the platform.

In what follows, we consider small-angle swings only. Even so, the problem is nonlinear due to the impulsive kicks. Between kicks the dynamics is linear, however, and the motion can be decomposed into a superposition of independent normal mode oscillations. We exploit this below in deriving a Poincaré map, alternately applying the normal mode evolution and the instantaneous effect of the kicks.

Before turning to a derivation of the iterative map, we pause to present a simple explanation of Huygens's observation. Introducing sum and difference variables, $\sigma = \phi_1 + \phi_2$ and $\delta = \phi_1 - \phi_2$, equations (4.4) and (4.5) become, for small oscillations and between kicks,

$$\delta'' + 2\gamma\delta' + \delta = 0, \tag{4.7}$$

$$\sigma'' + 2\gamma\sigma' + \sigma = -2Y'', \tag{4.8}$$

$$Y'' + 2\Gamma Y' + \Omega^2 Y = -\mu\sigma''. \tag{4.9}$$

Only the sum coordinate couples to the platform motion. Thus, the damping in the platform affects σ but not δ. To take the most extreme situation, if the pendulums were free of friction (i.e. $\gamma = 0$), the coordinate σ would still damp out; only δ survives, and this corresponds to pure anti-phase motion, just as Huygens observed.

This argument is instructive, and has the essential ingredients, but is incomplete since it ignores the energy input altogether. Without the kicks, the amplitude of the surviving (anti-phase) oscillations would depend on the initial conditions (contrary to observations) and for nearly in-phase initial conditions the anti-phase amplitude would be so small that the clock escapement would not engage, so that the anti-phase state would be unsustainable even in principle.

Nevertheless, the normal modes play a central role in the analysis that follows. Using the (complex) notation $\delta(t) = \delta_j e^{i\omega_j t}$, $\sigma(t) = \sigma_j e^{i\omega_j t}$ and $Y(t) = Y_j e^{i\omega_j t}$ to define the jth mode, we can determine the three mode frequencies ω_j and the corresponding mode coordinates Ψ_j. One mode follows from the decoupling of the difference coordinate:

$$\omega_1 = 1 + i\gamma, \qquad \Psi_1 = (\delta, \sigma, Y) = (1, 0, 0). \tag{4.10}$$

This describes pure anti-phase motion with decay rate $\mathrm{Im}(\omega_1) = \gamma$. Here and in what follows, we will assume for convenience that the damping is weak ($\gamma \ll 1$) and so neglect terms of order γ^2. The exact expressions for the other two modes are cumbersome, but for our purposes it is enough to develop them as a power series in

the mass ratio μ. We find

$$\omega_2 = 1 + i\gamma + \mu(1 + 2i(\gamma + \Gamma)), \qquad \Psi_2 = (0, 1, \mu d[1 - 2id(\Gamma - \Omega^2\gamma)]) \qquad (4.11)$$

and

$$\omega_3 = \Omega + i\Gamma + O(\mu), \qquad \Psi_3 = (0, 2\Omega^2, 1) + O(\mu), \qquad (4.12)$$

where $d^{-1} = \Omega^2 - 1$, and we have written these in a form suitable for the case where the platform is underdamped ($\Omega > \Gamma$). In fact, this is not a necessary assumption. We only want to avoid the resonant case $\Omega = 1$ when the platform frequency matches the pendulum frequency, so we assume either the frequencies do not match or the platform motion is overdamped.

Consideration of the mode structure allows us to simplify our analysis. First, since we want to consider the situation where the platform has 'imperceptible movements', Y is small. But the only linear combinations of the three modes $\sum_j c_j \Psi_j$ which yield a small value for Y have an equally small amount of the third mode, $c_3/c_2 \sim O(\mu)$. This means that the third mode is barely excited. Second, the remaining modes Ψ_1 and Ψ_2 are only $O(\mu)$ different from δ and σ, respectively. Thus, if a kick from the escapement mechanism boosts the value of ϕ_1, say, then to leading order in μ it affects modes Ψ_1 and Ψ_2 and not Ψ_3.

Together, these observations allow us to ignore the third mode, thereby reducing the problem to two degrees of freedom. We now proceed to construct a Poincaré map in the reduced, four-dimensional phase space, which is spanned by the coordinates $(\phi_1, \phi_1', \phi_2, \phi_2')$. Our strategy is to exploit the weakness of the damping and coupling. During one oscillation, we imagine that each pendulum executes a nearly free harmonic orbit, and then compute the small changes due to the damping and driving. Thus, we define

$$\phi_j = A_j \sin(\tau + \alpha_j), \quad j = 1, 2, \qquad (4.13)$$

where the iterative map describes updates in the amplitudes A_j and phases α_j. In the phase plane for each pendulum, one can picture the free orbit as uniform motion around the circle of radius A_j, except that when it reaches the positions $\phi_j = \Phi$ when $\phi_j' > 0$ and $\phi_j = -\Phi$ when $\phi_j' < 0$, the pendulum suddenly changes sign due to the kick from the clock mechanism (see figure 5). During the remaining motion there is energy loss due to friction.

The map we will derive considers the moment when the first pendulum passes through its lowest point moving to the right, so the Poincaré section is $\phi_1 = 0$, $\phi_1' > 0$. We consider in turn the effect due to (1) the damping and (2) the four impacts with the clock mechanisms (two impacts per pendulum per cycle).

(a) Damping

The effect of damping is most easily expressed by using the normal mode coordinates, which are to leading order just the sum and difference combinations σ and δ. Introducing the 'polar' representation corresponding to equation (4.13), we can write

$$\sigma = A_+ \sin(\tau + \alpha_+), \qquad (4.14)$$

$$\delta = A_- \sin(\tau + \alpha_-), \qquad (4.15)$$

where

$$A_\pm^2 = A_1^2 + A_2^2 \pm 2A_1 A_2 \cos(\alpha_1 - \alpha_2), \qquad (4.16)$$

$$\tan \alpha_\pm = \frac{A_1 \sin \alpha_1 \pm A_2 \sin \alpha_2}{A_1 \cos \alpha_1 \pm A_2 \cos \alpha_2}, \qquad (4.17)$$

and so

$$4A_j^2 = A_+^2 + A_-^2 \pm 2A_+ A_- \cos(\alpha_+ - \alpha_-), \qquad (4.18)$$

$$\tan \alpha_j = \frac{A_+ \sin \alpha_+ \pm A_- \sin \alpha_-}{A_+ \cos \alpha_+ \pm A_- \cos \alpha_-}, \qquad (4.19)$$

where the upper signs correspond to $j = 1$ and the lower signs to $j = 2$.

The normal modes evolve independently, with the real and imaginary parts of each mode frequency determining the time variation of the mode amplitude and phase, respectively. If we denote the mode frequencies by ω_+ and ω_- for in-phase and anti-phase, respectively, over one oscillation we have $A_+ \to \xi A_+$, $A_- \to \nu A_-$, and $(\alpha_+ - \alpha_-) \to (\alpha_+ - \alpha_-) + \beta$, where the constants ξ, ν and β are

$$\xi = e^{-2\pi \operatorname{Im} \omega_+}, \qquad (4.20)$$

$$\nu = e^{-2\pi \operatorname{Im} \omega_1}, \qquad (4.21)$$

$$\beta = 2\pi \operatorname{Re}(\omega_+ - \omega_-). \qquad (4.22)$$

One can work out what this corresponds to in terms of the variables $(A_1, A_2, \alpha_1, \alpha_2)$ using equations (4.18) and (4.19). Denoting the new values by a tilde, the result is

$$4\tilde{A}_1^2 = (\xi + \nu)^2 A_1^2 + (\xi - \nu)^2 A_2^2 + 2(\xi^2 - \nu^2)A_1 A_2 \cos \alpha + \beta 4\xi\nu A_1 A_2 \sin \alpha, \quad (4.23)$$

$$4\tilde{A}_2^2 = (\xi - \nu)^2 A_1^2 + (\xi + \nu)^2 A_2^2 + 2(\xi^2 - \nu^2)A_1 A_2 \cos \alpha - \beta 4\xi\nu A_1 A_2 \sin \alpha, \quad (4.24)$$

$$\tan \tilde{\alpha} = \frac{2\xi\nu[2A_1 A_2 \sin \alpha + \beta(A_1^2 - A_2^2)]}{(\xi^2 - \nu^2)(A_1^2 + A_2^2) + 2(\xi^2 + \nu^2)A_1 A_2 \cos \alpha}, \qquad (4.25)$$

where

$$\alpha = \alpha_1 - \alpha_2 \qquad (4.26)$$

and we have kept terms to first order in β. Physically, β is the coupling-induced frequency shift between the otherwise degenerate normal modes, which of course is small for small coupling. Subtracting the old values from the new ones, we get

$$\Delta_d A_j = \tilde{A}_j - A_j, \qquad (4.27)$$

$$\Delta_d \alpha = \tilde{\alpha} - \alpha, \qquad (4.28)$$

where the notation Δ_d indicates the changes due to damping in the amplitudes and the phase differences.

(b) Impacts

Since the impacts 'truncate' the free orbit near the turning points, the pendulum periods are less than 2π (figure 5). This amounts to advancing the phases α_j. The situation is particularly simple if considered in terms of the single-oscillator phase space: the time taken to traverse the truncated orbit is directly proportional to the
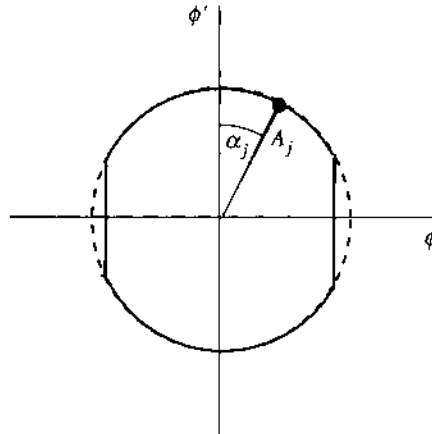
Figure 5. Phase portrait of single 'free' orbit truncated at $\phi_j = \pm\Phi$.

perimeter of the truncated circle, so that it takes a time $T = 4\arcsin(\Phi/A_j)$ for the jth pendulum to return to the section. With Δ_i indicating the changes due to the impacts, the change in α_j is

$$\Delta_i\alpha_j = 2\pi - 4\arcsin(\Phi/A_j), \quad j = 1, 2, \tag{4.29}$$

so that

$$\Delta_i\alpha = \Delta_i\alpha_1 - \Delta_i\alpha_2. \tag{4.30}$$

The effect on the amplitudes can be calculated by energy considerations. Noting that $\phi_j^2 + \phi_j'^2 = A_j^2$ is constant over the unperturbed orbit, the angular speed at $\phi_j = \pm\Phi$ is

$$|\phi_j'| = \sqrt{A_j^2 - \Phi^2}. \tag{4.31}$$

Applying the impulse rule equation (4.6) twice,

$$|\phi_j'| \to (1 - c)[(1 - c)|\phi_j'| + \epsilon] + \epsilon, \tag{4.32}$$

which gives the angular speed the instant after the second kick. Using equation (4.31) again gives the new amplitude, and thus the change due to the impacts:

$$\Delta_i A_j = \left\{ \Phi^2 + [(1 - c)^2\sqrt{A_j^2 - \Phi^2} + (2 - c)\epsilon]^2 \right\}^{1/2} - A_j. \tag{4.33}$$

These changes in phase and amplitude apply only if the amplitude is big enough to trigger the escapement, i.e. only if $A_j > \Phi$.

(c) *Analysis of the map*

Together, the contributions from the impacts and the damping give a three-dimensional return map for the coordinates (A_1, A_2, α):

$$A_1 \to A_1 + \Delta_i A_1 + \Delta_d A_1, \tag{4.34}$$

$$A_2 \to A_2 + \Delta_i A_2 + \Delta_d A_2, \tag{4.35}$$

$$\alpha \to \alpha + \Delta_i\alpha + \Delta_d\alpha. \tag{4.36}$$

We can identify three fixed points, all of which have equal amplitudes ($A_1 = A_2$). One is the trivial solution $A_1 = A_2 = 0$. To find the other two, note first that if $A_1 = A_2$ then $\Delta_i \alpha_1 = \Delta_i \alpha_2$ from equation (4.29) and $\Delta_i A_1 = \Delta_i A_2$ from equation (4.33). Meanwhile, in equations (4.23) and (4.24), setting $\alpha = 0$ or π and $A_1 = A_2$ implies $\tilde{A}_1 = \tilde{A}_2$, while taking $A_1 = A_2$ and the limit $\alpha \to 0$ or π in equation (4.25) yields $\tilde{\alpha} \to 0$ or π, respectively. Thus, we have two non-trivial fixed points, one with $\alpha = 0$ and the other with $\alpha = \pi$. These are the in-phase and anti-phase states, respectively.

Before we discuss the behaviour of the full three-dimensional map, it is useful to consider the special case $A_1 = A_2 > \Phi$ and $\beta = 0$. We can get a fairly complete picture in this case. The subspace $A_1 = A_2$ is invariant and contains the fixed points identified above. Moreover, the phase difference α obeys its own map. From equation (4.29) we see that α is unchanged due to the impulsive kicks, and from equation (4.25) that the amplitudes cancel out, leading us to the one-dimensional map

$$\tilde{\alpha} = \arctan\left\{ \frac{2\xi\nu\sin\alpha}{(\xi^2 - \nu^2) + (\xi^2 + \nu^2)\cos\alpha} \right\}. \tag{4.37}$$

For any ξ, ν, there are exactly two fixed points, $\alpha = 0$ and π. These are just the non-trivial fixed points already identified. By looking at the slope of this map one readily shows that $\alpha = 0$ is locally unstable and $\alpha = \pi$ is locally stable, for all allowed ξ, ν.

There is an alternative way to analyse the equal-amplitude case which allows us to make a stronger statement about the stability of the anti-phase state. The argument focuses directly on the mode energies, which gives it a certain conceptual advantage. The mode energies are proportional to the squared amplitudes $A_\pm^2$. Setting $A_1 = A_2 = A$ in equation (4.16) yields

$$A_\pm^2 = 2A^2(1 \pm \cos(\alpha_1 - \alpha_2)). \tag{4.38}$$

Now, we have established (cf. equation (4.29)) that if $A_1 = A_2$, the impulses do not affect α. Thus, if the impulse causes an amplitude change $A \to A + \Delta A$, we have from equation (4.38)

$$A_\pm \to \frac{A + \Delta A}{A} A_\pm,$$

which says that A_+ and A_- are scaled by the same factor. Meanwhile, frictional damping also acts to scale A_+ and A_-:

$$A_+ \to \xi A_+, \qquad A_- \to \nu A_-,$$

where $0 \leqslant \xi < \nu \leqslant 1$. Taken together, the two contributions yield the map

$$\tilde{A}_+ = \xi\left(1 + \frac{\Delta A}{A}\right) A_+, \tag{4.39}$$

$$\tilde{A}_- = \nu\left(1 + \frac{\Delta A}{A}\right) A_-. \tag{4.40}$$

Note that this does not give an explicit description of the system's evolution, since A itself is a dynamical variable. Nevertheless, it is enough to draw the strong conclusion that the anti-phase state is globally attracting (within the equal amplitude subspace). This follows because, since $\xi < \nu$, proportionately more energy is drained out of the

in-phase mode than is put into it, in all cases except if the system is perfectly in-phase (and so $A_- = 0$).

Let us return now to consider the full three-dimensional map. Numerical simulations of the three-dimensional map reveal that the anti-phase state and the trivial state are asymptotically stable, while the in-phase state is unstable, consistent with Huygens's observations (and ours). As already noted, β is the frequency difference between the two normal modes; when $\beta \neq 0$, the main effect is the introduction of beats, which eventually damp out (see figure 2). Because of these, even if the pendulums initially have the same amplitude, this property does not persist. Nevertheless, the beating merely introduces a transient which serves to decorate the main trends in the system's evolution, i.e. those trends which we previously deduced by setting $\beta = 0$, without affecting the long-term behaviour.

The map behaves very similarly to our experiments and Huygens's observations. Figure 2 shows a typical situation: even when started close to the in-phase state, the system evolves into the anti-phase state, with damped beating behaviour in both the amplitudes and the phase difference. More generally, the model qualitatively reproduces the important features of the experimental data, though there are some differences. The chief discrepancy is that the model shows a much smaller modulation of the amplitudes, a property that can be traced to the sharp impulse mechanism (see equation (4.6)).

This is not the end of the story, however. Simulations reveal another type of attracting state, where one pendulum oscillates but the other does not; we call this behaviour 'beating death' because beating plays an important role in determining the final dynamical state. Beating death happens when the pendulum amplitudes get very close to the escapement threshold Φ. If both pendulums have sub-threshold amplitudes, there is no energy input and the system is attracted to the trivial state $A_1 = A_2 = 0$. However, if the two amplitudes are slightly larger than Φ, the beating can introduce a large enough difference between the two so that the motion of one pendulum dies out while the other does not. This type of final state is also observed in our experiments when the coupling is sufficiently strong.

Drawing everything so far together, we find that depending on initial conditions the system ends up either in the anti-phase state or in beating death. The latter occurs more often the greater the coupling, all other parameters held fixed. We can estimate when we expect to observe beating death with significant probability by considering the in-phase solution (for which damping effects are greatest) with $A_1 = A_2$ and computing the value of the common value A: when this falls below Φ the motion cannot be sustained. This leads to the following condition for beating death:

$$\frac{1}{2\Phi}(2-c)^2\epsilon^2 - 2\pi\gamma - 4\pi\mu(\gamma + \Gamma) < 0. \tag{4.41}$$

The first term is the amplitude boost due to the clock mechanism (when $A = \Phi$), the rest is the amplitude loss due to friction in pendulum and platform. It is the μ-dependent term that is interesting from the point of view of Huygens's observations, since presumably his clocks were run under the condition that, in isolation, each clock maintains its oscillations. We see plainly that for large enough μ the condition for quiescence is satisfied.

Finally, we consider the effect of non-identical clocks. With identical pendulums, the anti-phase state is attracting for arbitrarily small values of μ. However, in general
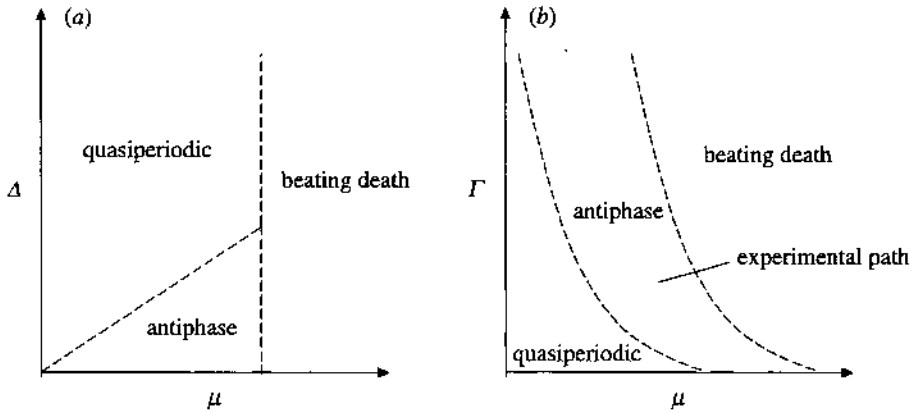
Figure 6. Phase diagrams summarizing theoretical analysis:
(a) Δ-μ parameter plane; (b) Γ-μ parameter plane.

one expects that two oscillators with different natural frequencies will not frequency lock unless the coupling exceeds some minimum threshold value. We can get an estimate of this threshold by the following argument. Assuming that the amplitudes are very nearly equal, and that the beating parameter β is sufficiently small that they stay nearly equal, the relative phase evolves according to the map (see equation (4.37))

$$\bar{\alpha} = \Delta + \arctan\left\{ \frac{2\xi\nu\sin\alpha}{(\xi^2 - \nu^2) + (\xi^2 + \nu^2)\cos\alpha} \right\}, \tag{4.42}$$

where a constant Δ has been added to account for the difference in pendulum frequencies. (More specifically, if these frequencies differ by an amount ρ, then in the uncoupled case α advances by an amount ρT, where T is the mean period.) As the detuning is increased, the $\alpha = 0$ fixed point shifts up and the $\alpha = \pi$ fixed point shifts down, until they coincide at the critical detuning Δ_c, beyond which the pendulums are not frequency locked. Since both ξ and ν differ only a little from unity, we can find Δ_c by setting $\alpha = \pi/2$ in equation (4.42), with the result

$$\Delta_c \approx \frac{\xi - \nu}{\nu}. \tag{4.43}$$

For example, taking $\Omega^2 \ll 1$, this becomes

$$\Delta_c = 4\pi\mu(\Gamma + \gamma). \tag{4.44}$$

5. Discussion and serendipity

Figure 6 summarizes our theoretical results. The figure depicts which of the three types of attracting states predominate as a function of system parameters. The state labelled 'quasiperiodic' refers to the case where the pendulums run at different frequencies. Near each boundary the system can end up in one or other state depending on initial conditions. We have made two plots in order to piece together the full picture as a function of the three key parameters. In figure 6a, we hold the platform damping Γ fixed, and vary the detuning Δ and coupling strength μ. The anti-phase

regime exists only if the detuning is small enough, consistent with our experimental observations. Figure 6*b* shows the situation for fixed Δ, as a function of Γ and μ. The anti-phase state sits in between the quasiperiodic and 'death' states. It is worth noting that as we vary the platform weight M, the path followed by our experiments is not strictly parallel to the μ-axis because varying M also mildly affects the dimensionless damping Γ (figure 6*b*).

Our results suggest that Huygens's observation of 'sympathy' depended on both talent and luck. The clock boxes were weighted by some 100 lb of lead in order to keep them upright in stormy seas. If they had not been, the mass ratio would have been too large, making the coupling too strong, and eventually stopping the clocks. Neither would his observation have been possible if the coupling was too weak, since the small but inevitable difference in the clock frequencies would prevent frequency locking. Only clocks with sufficiently close frequencies could fall into anti-phase lock-step. As it happened, Huygens's own inventions—and the clockmaker S. Oosterwijck's craftsmanship—made such exquisite matching possible.

References

Birch, T. 1756 *The history of The Royal Society of London for improving of natural knowledge, in which the most considerable of those papers communicated to the Society, which have hitherto not been published, are inserted in their proper order, as a supplement to the Philosophical Transactions*, vol. 2, pp. 19, 21, 23–24. London: Johnson. (Reprint 1968.)

Blekhman, I. I. 1988 *Synchronization in science and technology*. New York: ASME.

Britten, F. J. 1973 *Britten's old clocks and watches and their makers; a historical and descriptive account of the different styles of clocks and watches of the past in England and abroad containing a list of nearly fourteen thousand makers*. London: Methuen.

Burke, J. 1978 *Connections*. Boston: Little and Brown.

Golubitsky, M., Stewart, I., Buono, P.-L. & Collins, J. J. 1999 Symmetry in locomotor central pattern generators and animal gaits. *Nature* **401**, 693–695.

Heiskanen, W. A. & Vening Meinesz, F. A. 1958 *The Earth and its gravity field.* McGraw-Hill.

Huygens, C. 1669 Instructions concerning the use of pendulum-watches for finding the longitude at sea. *Phil. Trans. R. Soc. Lond.* **4**, 937.

Huygens, C. 1893 *Oeuvres complètes de Christiaan Huygens*, vol. 5, pp. 241–262. The Hague: Martinus Nijhoff. (Includes works from 1665.)

Huygens, C. 1932 *Oeuvres complètes de Christiaan Huygens*, vol. 17, pp. 156–189. The Hague: Martinus Nijhoff. (Includes works from 1651–1666.)

Huygens, C. 1986 *Christiaan Huygens's the pendulum clock or geometrical demonstrations concerning the motion of pendula as applied to clocks* (translated by R. Blackwell). Ames, IA: Iowa State University Press.

Korteweg, D. J. 1906 *Les horloges sympathiques de Huygens*. Archives Neerlandaises, sér. II, tome XI, pp. 273–295. The Hague: Martinus Nijhoff.

Landes, D. S. 1983 *Revolution in time: clocks and the making of the modern world.* Cambridge, MA: Belknap, Harvard University Press.

Lepschy, A. M., Mian, G. A. & Viaro, U. 1992 Feedback control in ancient water and mechanical clocks. *IEEE Trans. Educ.* **35**, 3–10.

Liao, P. & York, R. A. 1993 A new phase-shifterless beam-scanning technique using arrays of coupled oscillators. *IEEE Trans. Microwave Theory Techniques* **41**, 1810–1815.

Rawlings, A. L. 1944 *The science of clocks and watches.* New York: Pitman.

Rodriguez, E., George, N., Lachaux, J.-P., Martinerie, J., Renault, B. & Varela, F. J. 1999 Perception's shadow: long-distance synchronization of human brain activity. *Nature* **397**, 430–433.

Strogatz, S. H. & Stewart, I. 1993 *Scient. Am.* **269**, 102.

Yoder, J. G. 1990 *Unrolling time: Christiaan Huygens and the mathematization of nature.* Cambridge University Press.